Scientific Contributions Oil & Gas, Vol. 44. No. 2, August 2021: 83 - 95

SCIENTIFIC CONTRIBUTIONS OIL AND GAS
Reserach and Development Centre for Oil & Gas Technology
"LEMIGAS"

Journal Homepage:http://www.journal.lemigas.esdm.go.id
ISSN: 2089-3361, e-ISSN: 2541-0520

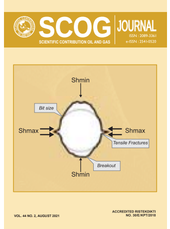

In Situ Stress and Stress Regime in the Offshore Part of the Northeast Java Basin

Agus M. Ramdhan
Applied Geology Research Group, Faculty of Earth Sciences and Technology,
Bandung Institute of Technology, Jl. Ganesa No. 10, Bandung, Indonesia
Corresponding author: agusmr@gl.itb.ac.id

Manuscript received: May, 28th 2021; Revised: July, 22nd 2021
Approved: August, 30th 2021; Available online: September, 2nd 2021

ABSTRACT - In situ stress is important in the petroleum industry because it will significantly enhance our understanding of present-day deformation in a sedimentary basin. The Northeast Java Basin is an example of a tectonically active basin in Indonesia. However, the in situ stress in this basin is still little known. This study attempts to analyze the regional in situ stress (i.e., vertical stress, minimum and maximum horizontal stresses) magnitude and orientation, and stress regime in the onshore part of the Northeast Java Basin based on twelve wells data, consist of density log, direct/indirect pressure test, and leak-off test (LOT) data. The magnitude of vertical (S_v) and minimum horizontal (S_{hmin}) stresses were determined using density log and LOT data, respectively. Meanwhile, the orientation of maximum horizontal stress (S_{hmax}) was determined using image log data, while its magnitude was determined based on pore pressure, mudweight, and the vertical and minimum horizontal stresses. The stress regime was simply analyzed based on the magnitude of in situ stress using Anderson's faulting theory. The results show that the vertical stress (S_v) in wells that experienced less erosion can be determined using the following equation: $S_v = 0.7622z^{1.0201}$ where is in psi, and z is in ft. However, wells that experienced severe erosion have vertical stress gradients higher than one psi/ft ($S_v = 1.0599z^{0.9982}$). The minimum horizontal stress (S_{hmin}) in the hydrostatic zone can be estimated as $S_{hmin} = 1.0599z^{0.963}$, while in the overpressured zone, $S_{hmin} = 0.7446z^{1.0228}$. The maximum horizontal stress (S_{hmax}) in the shallow and deep hydrostatic zones can be estimated using equations: $S_{hmax} = 2.4193z0^{.9432}$ and $S_{hmax} = 2.4902z^{0.9396}$, respectively. While in the overpressured zone, $S_{hmax} = 67.743z^{0.5362}$. The orientation of S_{hmax} is ~NE-SW, with a strike-slip faulting stress regime.

Keywords: Northeast Java Basin, in situ stress, stress regime.

How to cite this article:

Agus M. Ramdhan, 2021, In Situ Stress and Stress Regime in the Offshore Part of the Northeast Java Basin, Scientific Contributions Oil and Gas, 44 (2) pp., 83-95.

INTRODUCTION

Knowledge of in situ stress is very important in hydrocarbon exploration to the production stage. It will provide a better understanding of present-day deformation. Binh, *et al.* (2007) summarized that in situ stress is the main control of borehole stability, reservoir drainage and flooding, fluid flow in fractured reservoirs, hydraulic fracturing, and fault seal breach.

The onshore part of the Northeast (NE) Java Basin is tectonically located in a very active region (Figure 1). However, there is still little known about the in situ stress in this basin. The in situ stress consists of three components, i.e., vertical stress, minimum horizontal stress, and maximum horizontal stress. This study aims to analyze the stress regime and the magnitude of these stresses in the onshore part of the Northeast Java Basin on a regional basis using data from twelve wells (Figure 2).

DATA AND METHODS

A. Geological Setting

1. Tectonic and Stratigraphy

The Northeast Java Basin is a back-arc basin, particularly during Neogene (Koesoemadinata, 2020). Physiographically, the basin can be divided into several zones (Figure 2).

The study area includes Rembang Zone, Randublatung Zone, and Dander High. The deepest part of this basin is the Kendeng zone, a folded thrust zone is indicated by a negative Bouguer gravity anomaly (Figure 2).

The stratigraphy of the Northeast Java Basin is shown in Figure 3. The oldest Cenozoic formation in this basin is the Ngimbang Formation, a syn-rift Middle Eocene–Early Oligocene deposit consists of lacustrine–deltaic sandstones and mudrocks in the lower part and deep marine mudrocks with turbidite sandstone intercalations in the upper part. It is one of the main reservoirs in the Northeast Java Basin. Meanwhile, the youngest sedimentary sequence is the Lidah Formation, which consists of clay deposited in an enclosed marine environment.

The tectonic phases of this basin can be divided into the following phases (Koesoemadinata, 2020):

- Pre-rift
- Extensional rifting with syn-rift deposition in Early Eocene to Early Oligocene
- Sag phase with post-rift stable shelf deposition in Late Oligocene to Early Miocene
- Compressional phase in Middle Miocene to present-day

During the compressional phase, the onshore Northeast Java and Madura zone was down-warped and integrated into the East Java back-arc basin as compressional forces took place (Koesoemadinata, 2020).

B. Data Availability

The main data used in this study consists of density log, direct/indirect pressure test, and leak-off test (LOT) from twelve wells, as can be seen in Table 1. Direct pressure test data was obtained from Repeat

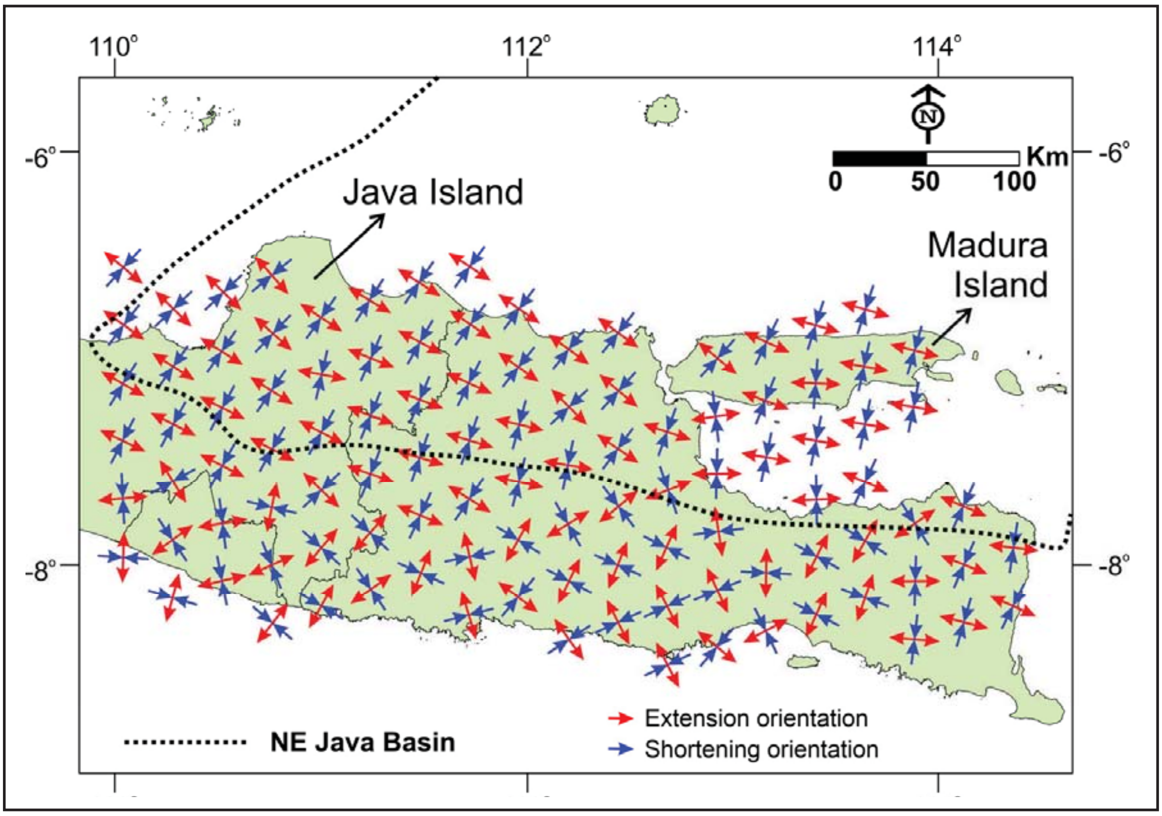

Figure 1
Map showing the orientation of extension and shortening of GPS strain
(modified from Gunawan and Widiyantoro, 2019) indicating active tectonic
in the onshore part of Northeast (NE) Java Basin (the basin boundary is from Koesoemadinata, 2020).

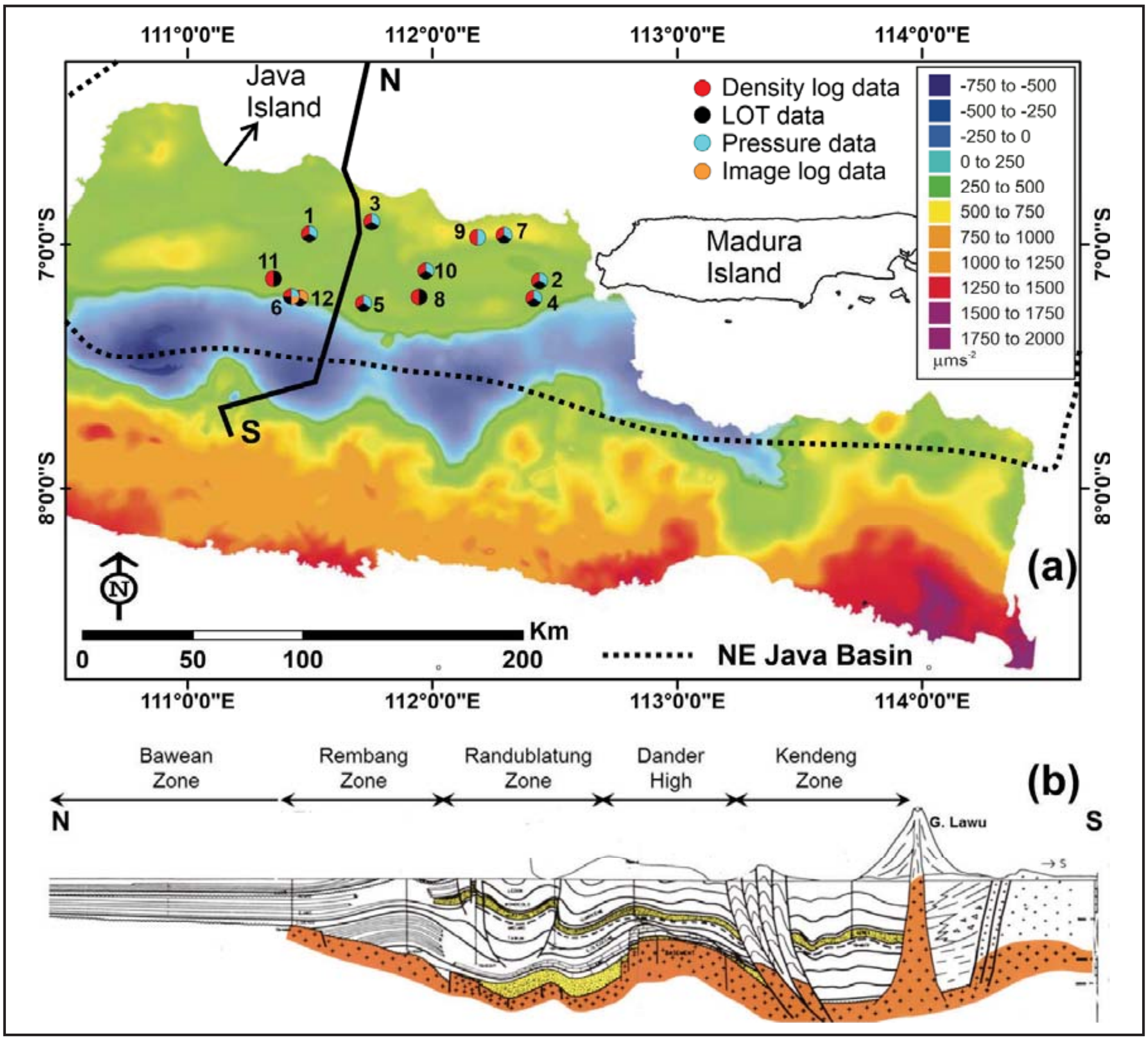

Figure 2
(a) Map showing Bouguer gravity anomaly (modified from Smyth *et al.*, 2008),
the twelve wells location, the available data, and the NE Java Basin boundary (Koesoemadinata, 2020).
(b) The cross-section showing the physiography of the NE Java Basin (Pertamina BPPKA, 1996).

Formation Tester (RFT), Modular Formation Tester (MDT), Reservoir Description Tool (RDT), and Drill Stem Test (DST). Meanwhile, the indirect pressure data were obtained based on mudweight used during the drilling and the drilling event (i.e., kick). Though most of the data are available, the number of the data for each well is limited. Therefore, a common regression analysis (power regression) was also carried out in this study.

C. Vertical Stress

Vertical stress at a given depth is simply stress due to its overlying sediment. Vertical stress in the onshore area is calculated by integrating density log as a function of depth by using this equation:

$$S_v = \int_0^z \rho_b(z) g dz \quad (1)$$

Where S_v is vertical stress, ρ_b is bulk density of sediments, g is gravitational acceleration, and z is depth.

The data source for obtaining vertical stress is the density log. Unfortunately, this log is not always available over the entire well interval, and its quality is very much affected by hole rugosity, as found in the study area. Most of the density logs of wells on the onshore part of the Northeast Java Basin are either not complete up to the surface or in poor condition due to the presence of hole enlargement caused by washout and caving, especially in the upper section where the lithology is dominated by unconsolidated material, and also in the limestone section. Caliper log was used to select the good density log. If the caliper log indicates the presence of hole enlargement, then the density log data were eliminated from further

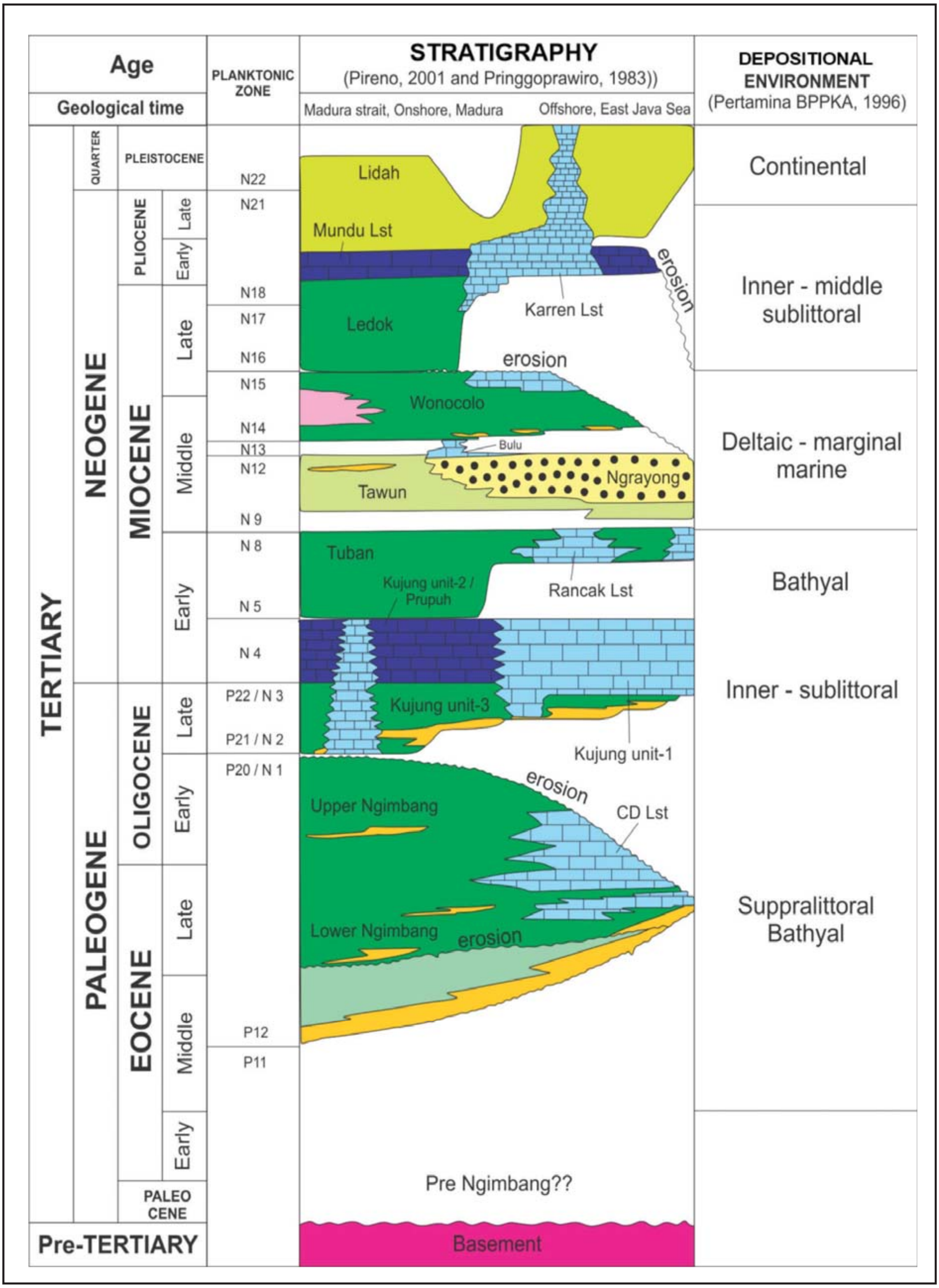

Figure 3
The stratigraphic column of the NE Java Basin
(modified after Mudjiono & Pireno (2001), Pringgoprawiro (1983), and Pertamina BPPKA (1996)).

Table 1
The summary of available data in this study.

Well	Density Log	Pressure Test	LOT
1	available	DST	available
2	available	RFT	available
3	available	Kick	available
4	available	RFT	available
5	available	RDT	available
6	available	MDT	available
7	available	DST	available
8	available	not available	available
9	available	DST	not available
10	available	RFT	available
11	available	not available	available
12	available	not available	available

analysis. The good density log data are interpolate to fill the missing or eliminated density data interval. Moreover, the density log was also manually filtered to remove the bad data reading indicated by the presence of spikes.

The most common assumption is that the average density of sediments is about 2.3 g/cm^3 down to the depth of 4-5 km. This density value gives an increase of vertical stress of 22.5 MPa/km or one psi/ft. This assumption can lead to some erroneous analyses requiring vertical stress as an input, such as pore pressure prediction and defining stress regime.

The more realistic equation relating vertical stress and depth is the power equation instead of the linear equation. This is because the density in the shallow section is relatively low, and then it is increasing through depth. It may reach a constant value at depth when the porosity approaches nearly zero.

By using this relation, the increase in vertical stress (S_v) through depth (z) follows this equation:

$$S_v = az^b \quad (2)$$

Where a and b are empirical constants obtained by fitted vertical stress with depth.

D. Minimum Horizontal Stress

The minimum horizontal stress can be determined using leak-off test (LOT) data. A summary of several pressure data obtained from LOT as shown in Figure 4 (White, *et al.*, 2002). Basically, the LOT test is performed by pumping the drilling mud into a well. In Figure 4, it can be seen that at the beginning of the test, the pressure inside the borehole will increase linearly as the mud volume is increasing. At Point B, there is a departure from the linearity, indicating that the elasticity of the rock has reached, and it is assigned as LOP (leak-off pressure). At the departure point, the pressure decreases a little bit compared if the linearity does not break up, indicating that the hydraulic fractures start to develop. At Point C, the formation breakdown (FBP) is reached, and in this stage, the fractures will propagate, and until a certain time, the pressure in the wellbore will be relatively constant because the mud will escape into the fractures. After this stage, the pump is turned off, and the pressure will drop. The point where the pressure starts to drop (Point D) is referred to as the instantaneous shut-in pressure (ISIP). The pressure inside the wellbore continues to decrease, and the fractures will close again. The fracture closure pressure (FCP) is determined by the ‘double tangent’ method, i.e., the cross-point between the ISIP line and the stabilized pressure line (point E). White, *et al.* (2002) stated that ISIP and FCP are the better estimates of the minimum horizontal stress than the LOP because the LOP is affected by stress perturbation and the hoop stress surrounding the wellbore when inducing or opening a fracture.

Yassir & Bell (1994) showed that the pore pressure relates to minimum horizontal stress. They demonstrated that the minimum horizontal stress increased in overpressured zones. Therefore, the pore

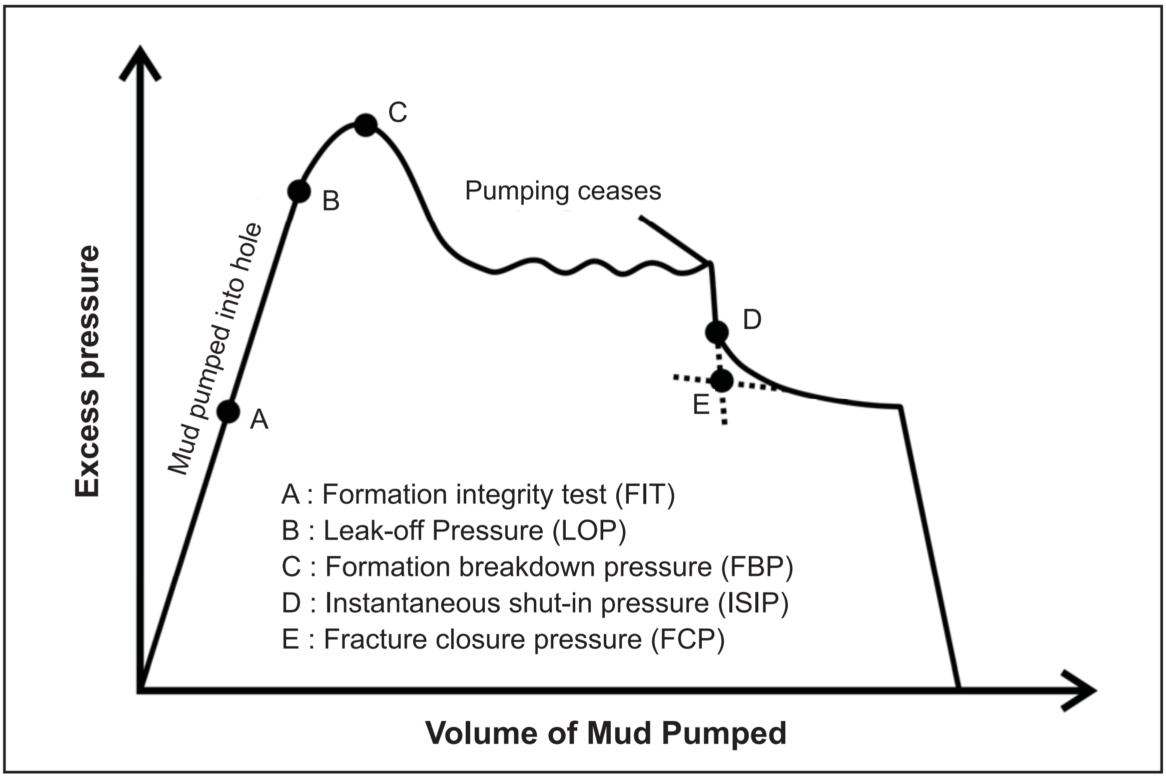

Figure 4
The schematic diagram of LOT (adapted from White *et al*., 2002).

pressure is analyzed before determining the value of this stress in this study.

Considering the pore pressure condition, the power regression of available LOT data from all wells was used as the proxy for minimum horizontal stress. This method has been used by Breckels & van Eekelen (1982) to establish minimum horizontal stress-depth relation in several sedimentary basins. This method is considered to be realistic in order to avoid factors affecting LOP as discussed above. The available LOT is then related with depth with the following power equation to estimate the minimum horizontal stress (S_{hmin}) value:

$$S_{hmin} = az^b \quad (3)$$

Where a and b are empirical constants obtained by fitted LOT data with depth.

Maximum Horizontal Stress

Different from the vertical and minimum horizontal stresses, the maximum horizontal stress (S_{Hmax}) cannot be determined directly. However, its orientation can be interpreted from earthquake data, borehole breakouts, and drilling-induced fractures (Binh, *et al*., 2011). In this study, the orientation is interpreted from available image log data. Moreover, the magnitude of S_{Hmax} at a given depth is estimated based on drilling -induced tensile fractures using the following equation (Zoback, 2007):

$$S_{Hmax} = 3S_{hmin} - P_b - P_p \quad (4)$$

Where S_{hmin} is the minimum horizontal stress, P_b is formation breakdown pressure (equal to mud pressure used for inducing tensile fractures), and P_p is pore pressure at the given depth. However, the drilling-induced tensile fractures data in this study are only available in two wells and in a very limited depth interval.

As the vertical and minimum horizontal stresses, the relation between the maximum horizontal stress (S_{Hmax}) and depth (z) is also determined using the power equation:

$$S_{Hmax} = az^b \quad (5)$$

Where a and b are empirical constants obtained by fitted with depth.

E. Stress Regime

The stress regime of the onshore part of the Northeast Java Basin was determined using Anderson's faulting theory. According to this theory, the stress regime can be classified into three based on the magnitude of the principal stresses (Table 2).

Jaeger & Cook (1979) showed that the value of S_1 (maximum principal stress) and S_3 (minimum principal stress) for a critically oriented fault at the frictional limit as:

$$\frac{S_1-P_p}{S_3-P_p} = [(\mu^2+1)^{0.5}+\mu^2] \quad (6)$$

Where P_p is pore pressure and μ is the coefficient of friction. For μ=0.6, the equation from Jaeger & Cook (1979) can be used to estimate the upper bound of in situ stresses using the following equation (Zoback, 2007):

$$\frac{S_v-P_p}{S_{hmin}-P_p} = 3.1 \text{ for normal faulting} \quad (7)$$

$$\frac{S_{Hmax}-P_p}{S_{hmin}-P_p} = 3.1 \text{ for strike-slip faulting} \quad (8)$$

$$\frac{S_{Hmax}-P_p}{S_v-P_p} = 3.1 \text{ for reverse faulting} \quad (9)$$

RESULTS AND DISCUSSION

A. Vertical Stress

As mentioned before, the first thing to do in constructing vertical stress is editing the density log

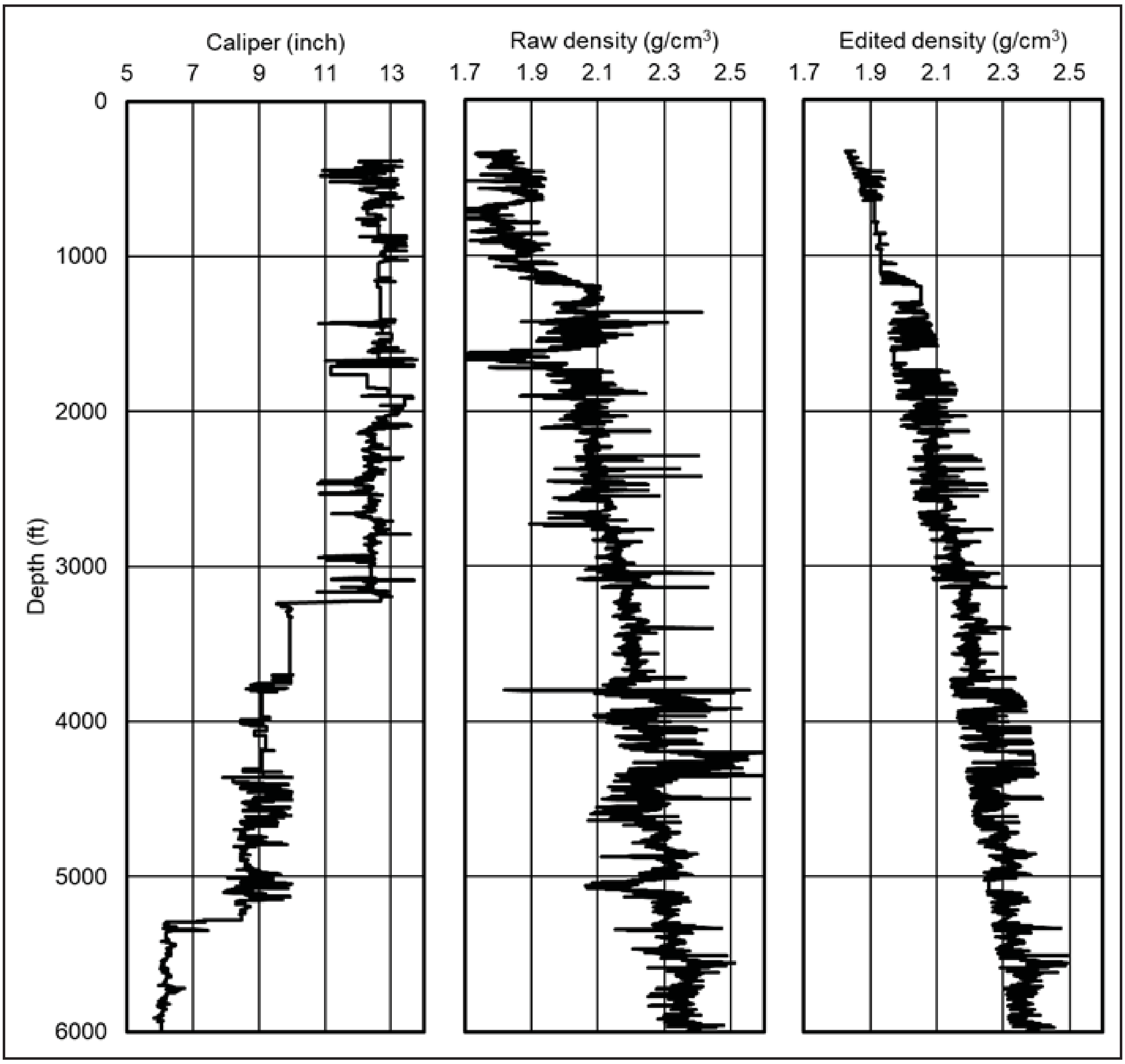

Figure 5
An example of density log editing from well number 4. It can be seen that the edited density log shows a consistent increase of density value through depth.

based on the caliper log, and filtering it manually for unrealistic values (spikes). An example of density editing is shown in Figure 5. The data is taken from well number 4. The caliper log indicates a good hole condition in general, with some minor hole enlargement in several sections. The raw density data contain some spikes, either unreasonably high or unreasonably low. After editing some bad data points based on the above criteria, we have edited the density log as shown in the right panel of Figure 5.

By using eq. (1), the vertical stress for all wells in the study area is shown in Figure 6a. It can be seen that the vertical stress in the study area is less than one psi/ft, except for well numbers 7 and 9. These two wells have experienced severe erosion that the section with lower density values has been eroded. This is the best explanation for why the vertical stress exceeds the value of one psi/ft in those two wells. Accordingly, it can be inferred that the majority of the wells where the vertical stress is less than one psi/ft have escaped from severe erosion. Ignoring well numbers 7 and 9, the average vertical stress in the study area could be approached by the following equation:

$$S_v = 0.7622z^{1.0201} \quad (10)$$

Where S_v is in psi, and z is in ft.

B. Minimum Horizontal Stress

As mentioned before, the minimum horizontal stress was determined from LOT data by considering the pore pressure condition. Figure 6b shows the simplified pore pressure profile in the study area. As indicated by the pressure data, the pore pressure

Table 2
The stress regime determination (Zoback, 2007)

Stress Regime	Principal Stress		
	S_1	S_2	S_3
Normal faulting	S_v	S_{Hmax}	S_{hmin}
Strike-slip faulting	S_{Hmax}	S_v	S_{hmin}
Reverse faulting	S_{Hmax}	S_{hmin}	S_v

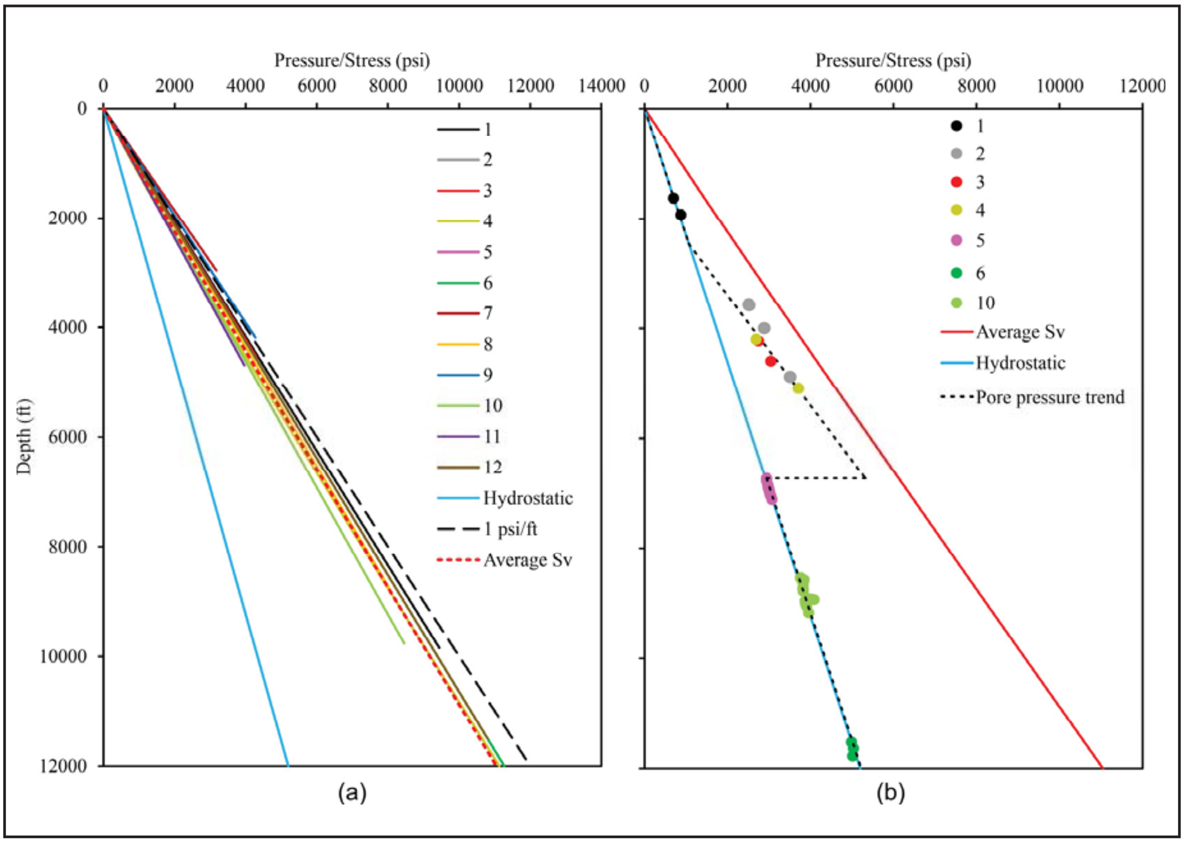

Figure 6
Diagram showing: (a) the vertical stress (S_v) in all wells and their average value (Average S_v), which is less than one psi/ft; (b) pore pressure trend based on available pressure data (colored circle).

from the surface to the depth of ~2,400 ft is hydrostatic. The overpressured zone is found from ~2,400 to ~6,750 ft. After that, the pore pressure is again in hydrostatic condition from ~6,750 ft to the total depth (TD) of wells in the study area.

It seems that the LOT data are not significantly scattered and in the range of nearly touching average vertical stress (Figure 7). The LOT data of well number 7 is greater than LOT data from other wells. It may also be related to severe erosion experienced by this well.

Ignoring LOT data of well number 7 and considering the pore pressure condition, the equations for relating minimum horizontal stress (S_{hmin}) with depth (z) in the study area are:

$$S_{hmin} = 1.0599z^{0.963} \quad (11)$$

$$S_{hmin} = 0.7446z^{1.0228} \quad (12)$$

Where S_{hmin} is in psi and is in ft. Eq. (11) is for hydrostatic zones, while eq. (12) is for the overpressured zone. The ratio of minimum horizontal stress and vertical stress (S_{hmin}/S_v) in hydrostatic zones, from 100 to 2,400 ft and from 6,750 to 12,000 ft, is in the range of 0.89 to 1.07 and 0.81 to 0.84, respectively. Meanwhile, the ratio of minimum horizontal stress and vertical stress (S_{hmin}/S_v) in the overpressured zone (2400 to 6750 ft) ranges from 0.99 to 1.

C. Maximum Horizontal Stress and Stress Regime

In order to estimate the magnitude of using eq. (4), the pore pressure and mud pressure used for inducing tensile fractures must be known. Figure 8 shows the estimated based on drilling-induced tensile fractures

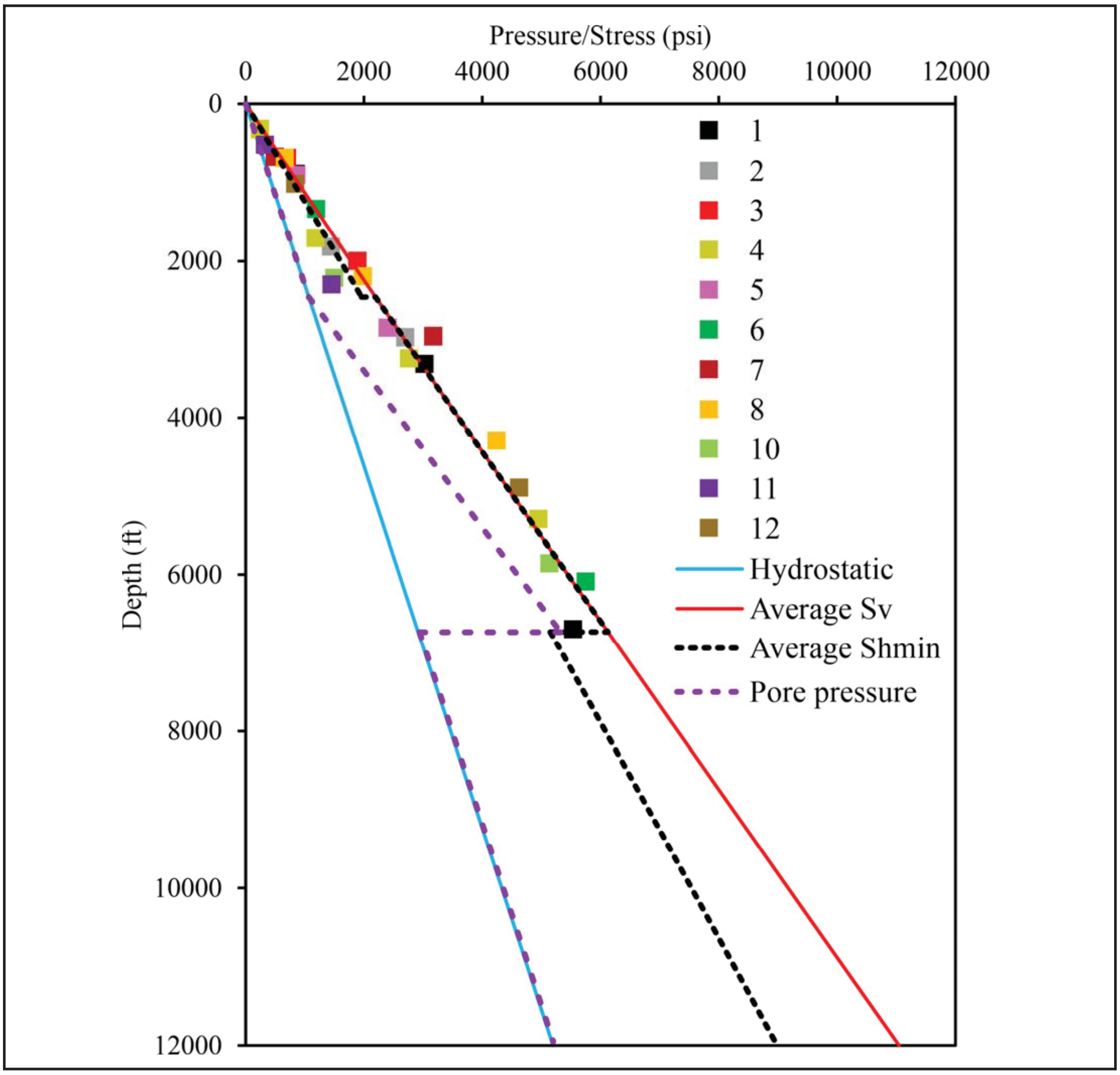

Figure 7
Diagram showing LOT data in all wells (colored box) and
the interpreted average minimum horizontal stress (Average S_{hmin}).

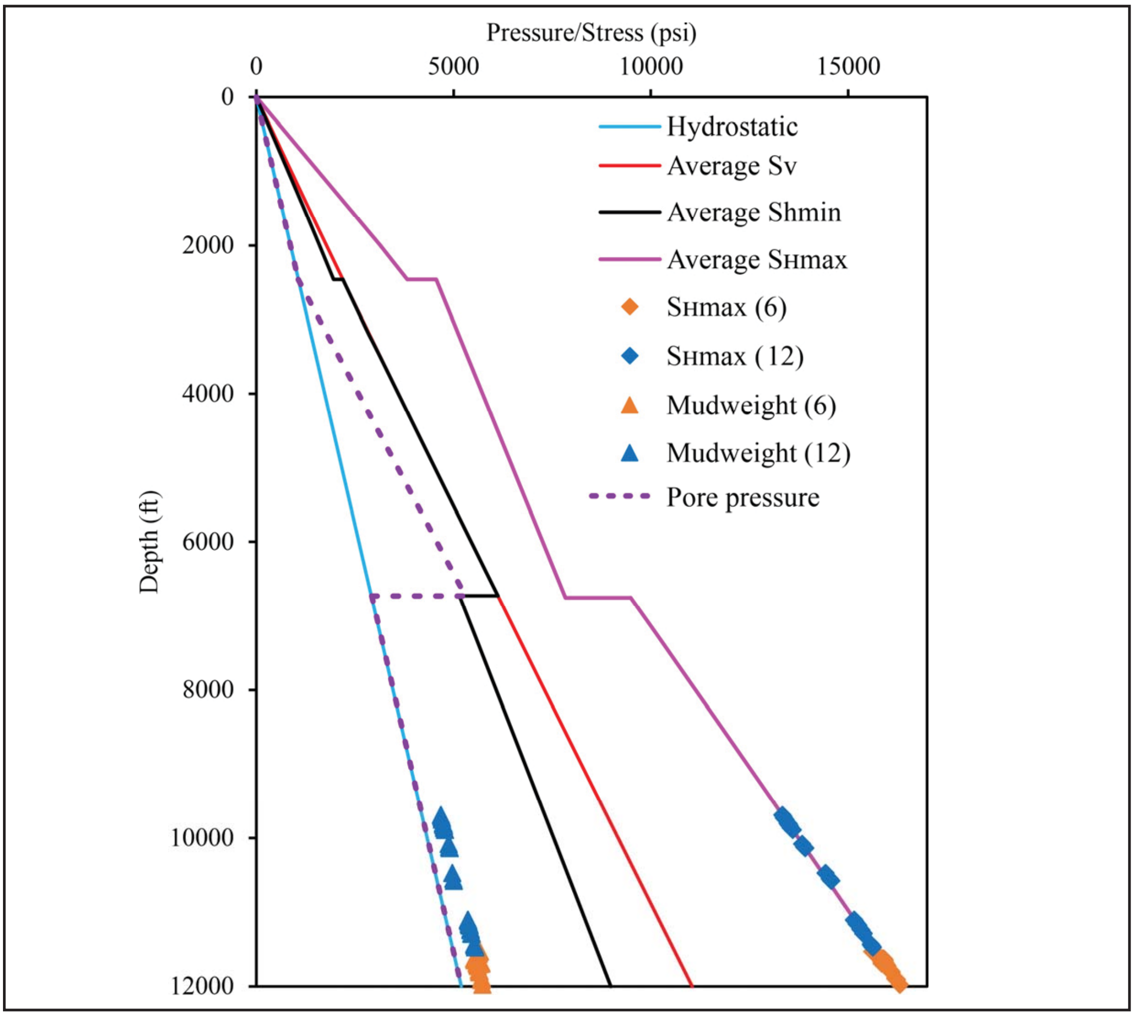

Figure 8
Diagram showing the interpreted average maximum horizontal stress (Average S_{Hmax}); numbers 6 and 12 indicate well numbers.

(blue and orange diamonds). It is clear that the stress regime is strike-slip faulting since $S_{Hmax} > S_v > S_{hmin}$. Therefore, eq. (8) can be used to estimate the in the depth interval where image log data are not available. Like the vertical and minimum horizontal stresses, the relation of S_{Hmax} and depth (z) can be written as the following equation:

$$S_{Hmax} = 2.4193z^{0.9432} \quad (13)$$

$$S_{Hmax} = 67.743z^{0.5362} \quad (14)$$

$$S_{Hmax} = 2.4902z^{0.9396} \quad (15)$$

Where S_{Hmax} is in psi and z is in ft. Eq. (13) is for the shallow hydrostatic zone (0 to 2,400 ft), eq. (14) is for the overpressured zone (2400 to 6,750 ft), while eq. (15) is for the deep hydrostatic zone (greater than 6,750 ft). The ratio of maximum horizontal stress and vertical stress (S_{Hmax}/S_v) in the hydrostatic zones, from 100 to 2,400 ft and from 6,750 to 12,000 ft, is in the range of 1.74 to 2.23 and 1.53 to 1.61, respectively. Meanwhile, The ratio of maximum horizontal stress and vertical stress in the overpressured zone (2400 to 6750 ft) ranges from 1.25 to 2.06.

The orientation of the maximum horizontal stress was analyzed based on image log data from two wells, i.e., well numbers 6 and 12 (Figure 9). Both image logs indicate that the orientation is ~NE-SW.

As already mentioned before, well numbers 7 and 9 experienced severe erosion that the section with lower density values has been eroded. This causes the vertical stress of these wells to exceed the value of one psi/ft, while the other wells do not. The average vertical stress (S_v) of these two wells could be approached by the following equation:

$$S_v = 1.0599z^{0.9982} \quad (16)$$

Where S_v is in psi, and z is in ft.

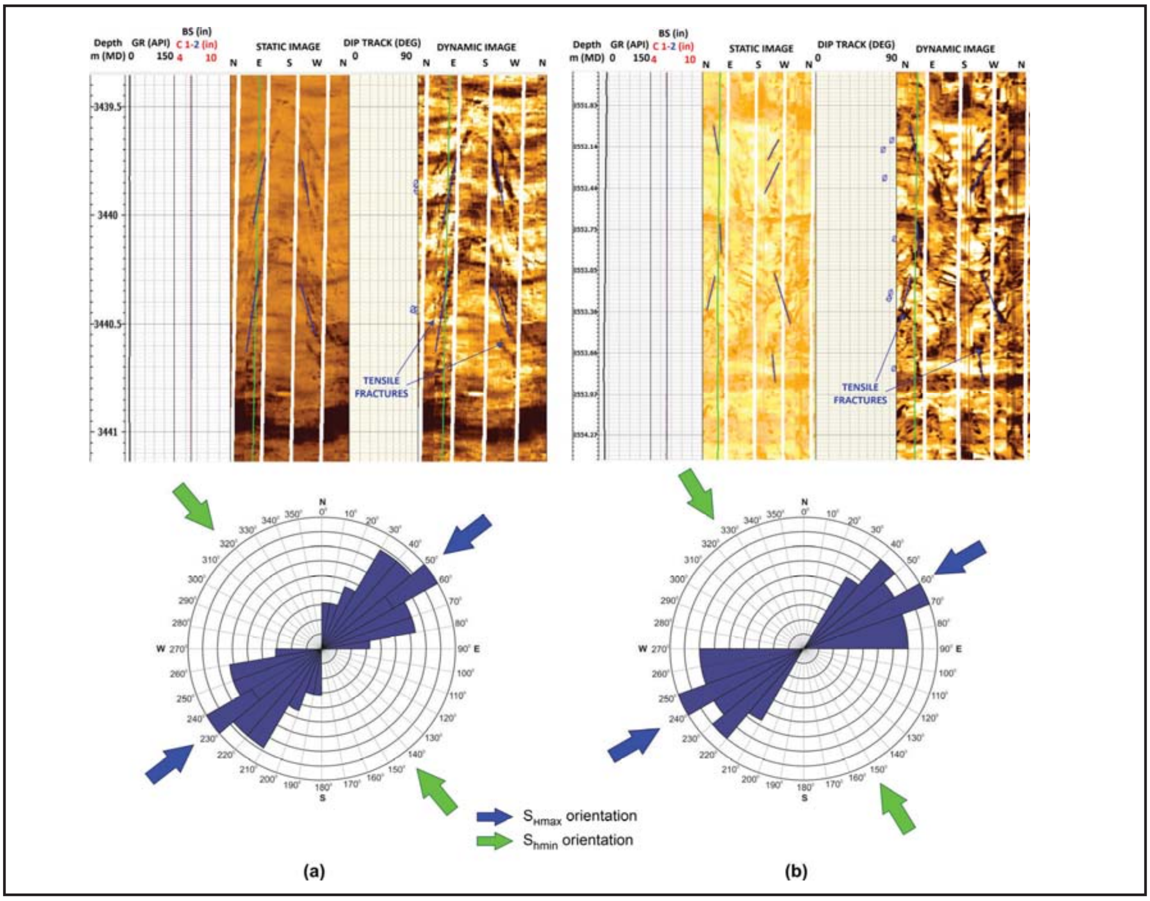

Figure 9
Image log and interpreted S_{Hmax} and S_{hmin} orientation in (a) well number 6 and (b) well number 12.

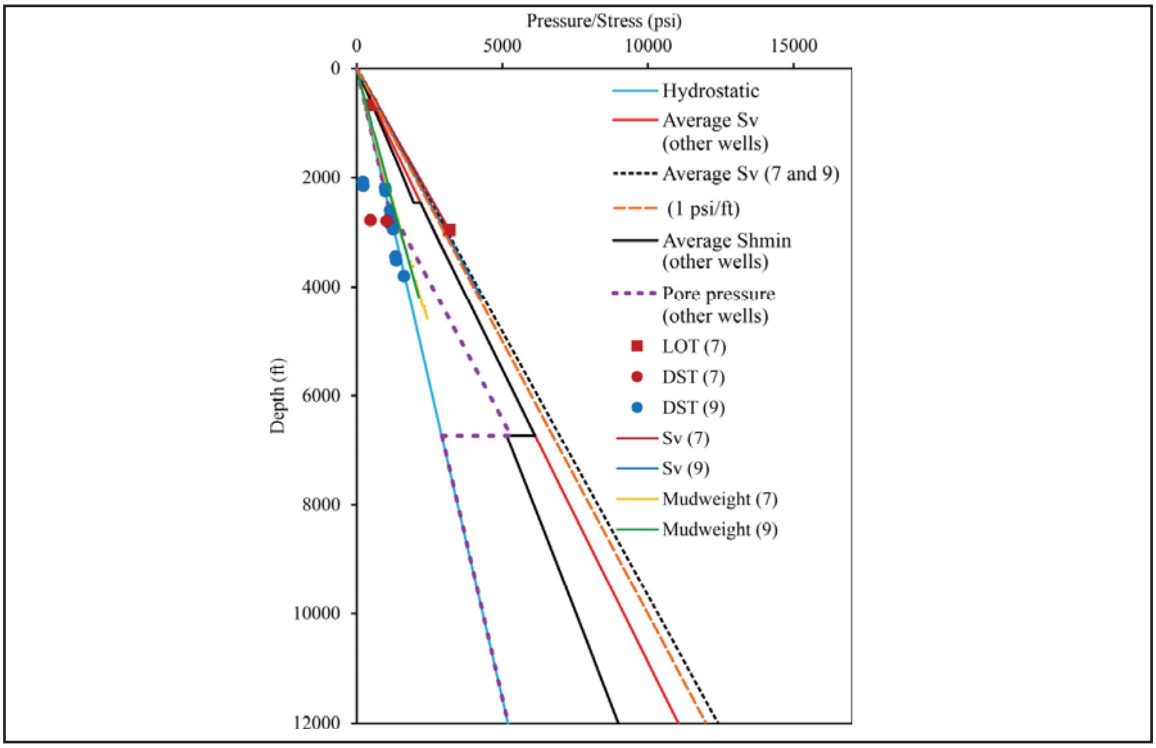

Figure 10
Diagram showing the available LOT, pressure test data (DST), and mudweight
in well numbers 7 and 9 compared to average S_v, S_{hmin}, and pore pressure in other wells.

Figure 10 shows that in these two wells, the reservoir pressure is mostly hydrostatic, though, in some depths, the reservoir pressure is depleted. Nevertheless, the mudweight used during drilling indicates that these two wells experienced slight overpressure. The LOT data of well number 7 still have the same pattern as the average S_{hmin} of other wells, i.e., in the overpressured zone, it coincides with the vertical stress.

Figures 7 and 10 show that there are no leak-off test data in the deep hydrostatic or pressure reversal zone. Thus, the in this interval can not be calibrated. However, Addis (1997) has demonstrated that pore pressure reduction is related to the significant decrease of minimum horizontal magnitude. Therefore, the real average S_{hmin} in this study could be lower than the interpreted average S_{hmin}.

CONCLUSIONS

In the onshore part of the Northeast Java Basin, the vertical stress (S_v) in wells that experienced less erosion is lower than one psi/ft, i.e., can be determined using the following equation: $S_v = 0.7622z^{1.0201}$, where S_v is in psi, and z is in ft. However, wells that experienced severe erosion have a vertical stress gradient higher than one psi/ft ($S_v = 1.0599z^{0.9982}$). The pore pressure condition in this basin can be generalized into three zones, shallow hydrostatic zone from the surface to ~2,400 ft, overpressured zone from ~2,400 to 6,750 ft, and deep hydrostatic zone in depths greater than ~6,750 ft. The minimum horizontal stress (S_{hmin}) in the hydrostatic zone can be estimated as $S_{hmin} = 1.0599z^{0.963}$, while in the overpressured zone, $S_{hmin} = 0.7446z^{1.0228}$. The maximum horizontal stress (S_{hmax}) in the shallow and deep hydrostatic zones can be estimated using equations: $S_{hmax} = 2.4193z^{0.9432}$ and $S_{hmax} = 2.4902z^{0.9396}$, respectively. While in the overpressured zone, $S_{hmax} = 67.743z^{0.5362}$.

The interpreted stress regime in the onshore part of the Northeast Java Basin is strike-slip faulting since the $S_{hmax} > S_v > S_{hmin}$. Moreover, the result of image log analysis indicates that the orientation of S_{hmax} is ~NE-SW.

ACKNOWLEDGEMENT

The authors would like to thank the reviewers who have provided valuable input on this paper. The author also thanks Mr. Arifin, M.T. for his contribution in preparing the images used in this paper.

GLOSSARY OF TERMS

Symbol	Definition	Unit
Bouguer gravity anomaly	the difference between measured gravity and known or modeled gravity values	
Caving	borehole collapse	
Hydrostatic	fluid pressure which is solely depended on the fluid density	
Kick	flux of fluid from formation into the borehole during drilling	
Maximum horizontal stress	the maximum stress in horizontal direction	
Minimum horizontal stress	the minimum stress in horizontal direction	
Mudweight	drilling mud with certain density	
Overpressure	fluid pressure that is greater than hydrostatic	
Pore pressure	the pressure of fluid in the pore space of rocks	
Vertical stress	stress that works in vertical direction due to the overlying material	
Washout	borehole enlargement	

REFERENCES

Addis, M., 1997. *The stress-depletion response of reservoirs.* San Antonio, Texas, Society of Petroleum Engineering (SPE), p. 55-65.

Binh, N. T. T., Tokunaga, T., Goulty, N.R., Son, H.P., & **Binh, M.V.**, 2011. Stress state in the Cuu Long and Nam Con Son basins, offshore Vietnam. *Marine and Petroleum Geology,* 28(5), pp. 973-979.

Binh, N. T. T., Tokunaga, T., Son, H. P. & **Binh, M.**, 2007. Present-day stress and pore pressure fields in the Cuu Long and Nam Con Son Basins, offshore Vietnam. *Marine and Petroleum Geology,* 24(10), pp. 607-615.

Breckels, I. & **van Eekelen, H.**, 1982. Relationship between horizontal stress and depth in sedimentary basins. *Journal of Petroleum Technology,* 34(09), p. 2191–2199.

Gunawan, E. & **Widiyantoro, S.**, 2019. Active tectonic deformation in Java, Indonesia inferred from a GPS-derived strain rate. *Journal of Geodynamics,* Volume 123, pp. 49-54.

Jaeger, J. & **Cook, N.**, 1979. *Fundamentals of Rock mechanics.* 2nd ed. New York: Chapman and Hall.

Koesoemadinata, R. P., 2020. *An Introduction into The Geology of Indonesia, Volume I: General Introduction & Part 1 Western Indonesia.* Bandung: Ikatan Alumni Geologi, Institut Teknologi Bandung.

Mudjiono, R. & **Pireno, G. E.**, 2002. *Exploration of the North Madura Platform, Offshore East Java, Indonesia.* Indonesia, Indonesian Petroleum Association.

Pertamina BPPKA, 1996. *Petroleum Geology of Indonesian Basins: Principles, Methods and Application.* Indonesia: Pertamina-BPPKA.

Pringgoprawiro, H., 1983. *Revisi Stratigrafi Cekungan Jawa Timur Utara dan Paleogeografinya.* Bandung: Institute of Technology Bandung. Unpublished.

Smyth, H. R., Hall, R. & **Nichols, G. J**., 2008. Cenozoic volcanic arc history of East Java, Indonesia: The stratigraphic record of eruptions on an active continental margin. *Geological Society of America Special Paper,* Volume 436, pp. 199-222.

White, A. J., Traugott, M. O. & **Swarbrick, R. E.**, 2002. The use of leak of test as mean of predicting minimum. *Petroleum Geoscience,* 8(2), pp. 189-193.

Yassir, N. A. & **Bell, J. S.,** 1994. Relationships between pore pressures, stresses and present-day geodynamics in the Scotian Shelf. *Offshore Eastern Canada,* Volume 78, p. 1863–1880.

Zoback, M. D., 2007. *Reservoir Geomechanics.* Cambridge: Cambridge.